

Electronic Supporting Information

Highly efficient CO₂ capture and conversion of a microporous acylamide functionalized *rht*-type metal-organic framework

Junxiong Liao,^{‡a} Wenjiang Zeng,^{‡a} Baishu Zheng,^{*a} Xiyang Cao,^a Zhaoxu Wang,^{*a} Guanyu Wang^a and Qingyuan Yang^{*b}

^aKey Laboratory of Theoretical Organic Chemistry and Function Molecule of Ministry of Education, Hunan Provincial Key Laboratory of Controllable Preparation and Functional Application of Fine Polymers, Hunan Provincial Key Laboratory of Advanced Materials for New Energy Storage and Conversion, School of Chemistry and Chemical Engineering, Hunan University of Science and Technology, Xiangtan 411201, China. E-mail: zbaishu@163.com (B. S. Zheng); hunst_chem@163.com (Z. X. Wang).

^bState Key Laboratory of Organic-Inorganic Composites, Beijing University of Chemical Technology, Beijing 100029, China. E-mail: qyyang@mail.buct.edu.cn (Q. Y. Yang).

[‡] These authors contributed equally to this work.

3. Synthesis of di-tert-butyl 5-iodoisophthalate (3)

SOCl₂ (10 mL, 137.5 mmol) was added dropwise to 5-iodoisophthalic acid **2** (0.7g, 2.4 mmol) with 100 μL DMF. The mixture was refluxed overnight and then the excess SOCl₂ was removed under vacuum. The resulting solid was dissolved in anhydrous THF and then tBuOK (1.1 g, 9.8 mmol) in 30 mL anhydrous THF was slowly added. After stirring for 24h at room temperature, the solvent was removed under vacuum, and the residue was washed with aqueous hydrochloric acid and water, and then filtered to give di-tert-butyl 5-iodoisophthalate **3** as a pale yellow solid (0.6g, 61.9 % yield). ¹H NMR (500 MHz, CDCl₃, δ ppm, Fig. S8a): 8.52 (s, 1H, ArH), 8.44 (s, 2H, ArH), 1.60 (m, 18H, COOtBu).

4. Synthesis of 3,5-di-tert-butyl 3',5'-dimethyl [1,1'-biphenyl]-3,3',5,5'-tetracarboxylate (4)

To a solution of di-tert-butyl 5-iodoisophthalate **3** (0.808 g, 2.0 mmol) in 60 mL toluene, 3,5-bis(methoxycarbonyl)phenylboronic acid (0.714 g, 3.0 mmol) in 12 mL ethanol and Na₂CO₃ (0.74 g, 7.0 mmol) in 4 mL water were successively added, after degassed using N₂ for 10 min, Pd(PPh₃)₄ (0.23 g, 0.2 mmol) was added. The resulting reaction mixture was stirred at 110 °C under N₂ atmosphere overnight. After removal of solvent under vacuum, the residue was dissolved in CH₂Cl₂ and then filtered. CH₂Cl₂ were removed under vacuum, and the crude product was purified by column chromatography on silica gel with dichloromethane as eluent to give 3,5-di-tert-butyl 3',5'-dimethyl [1,1'-biphenyl]-3,3',5,5'-tetracarboxylate **4** as a dark brown solid (0.58 g, 61.6 % yield). ¹H NMR (500 MHz, CDCl₃, δ ppm, Fig. S8b): 8.72 (s, 1H, ArH), 8.60 (s, 1H, ArH), 8.51 (s, 2H, ArH), 8.42 (s, 2H, ArH), 6.07 (s, 6H, COOCH₃), 8.51 (m, 18H, COOtBu).

5. Activation of HNUST-9

The solvent-exchanged HNUST-9 was prepared by immersing the as-synthesized sample in dry methanol for 48 hours to remove the non-volatile solvates (DMF and water), the extract was decanted every 8 hours and fresh methanol was replaced. The completely activated HNUST-9 sample was obtained by heating the solvent-exchanged sample at 100 °C under a dynamic high vacuum for 24 hours. During this time, the pale blue sample changed to a deep purple-blue colour (Fig. S3), indicative of the presence of open copper(II) sites. The completely-activated samples were moisture sensitive and a few minutes of exposure to air could change the sample's color back to pale blue. Anal. Calcd (Found) for [Cu₃(C₃₀H₁₄N₂O₁₄): C, 44.10 (44.06), H 1.739 (1.81), N 3.43 (3.38). Selected IR (KBr, cm⁻¹, Figure S4): 3416, 1652, 1620, 1559, 1370, 1276, 1106, 904, 755, 726, 692.

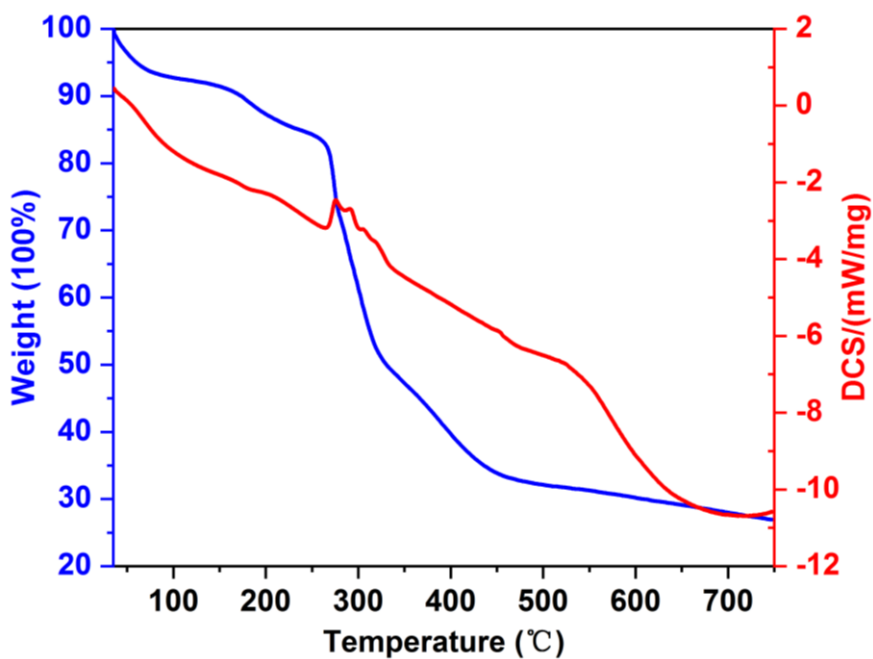


Fig. S1 TGA data of as-synthesized HNUST-9.

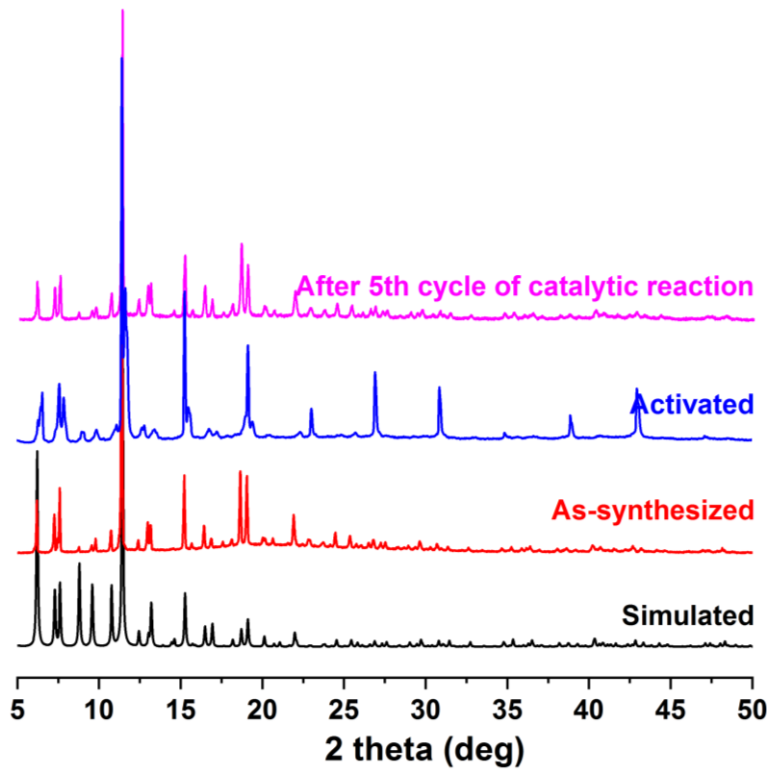


Fig. S2 PXRD patterns of HNUST-9: simulated, as-synthesized, activated, and after the 5th cycle of catalytic reaction, respectively.

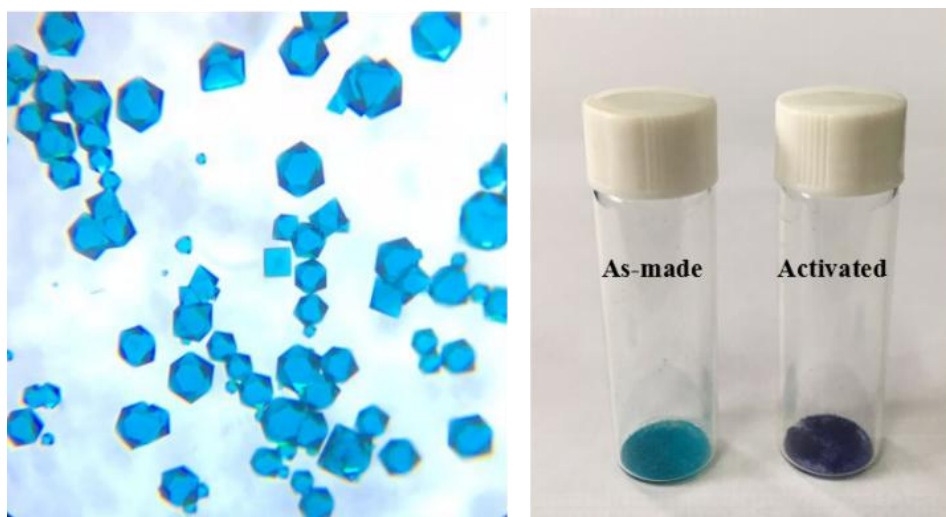


Fig. S3 Left) Photographic image of as-synthesized HNUST-9, the crystal size has been magnified about 80 times; Right) Visual color change of HNUST-9 upon activation.

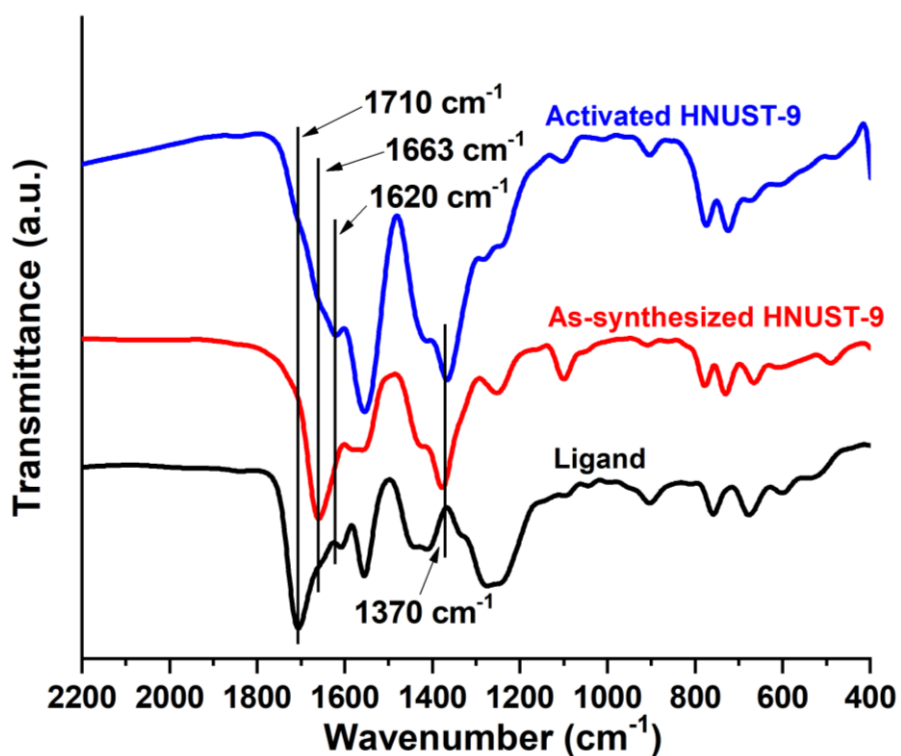


Fig. S4 The IR spectra for HNUST-9. a) Ligand; b) As-synthesized; and c) Activated HNUST-9. Note the absence of the vibration frequencies of the solvent DMF and methanol molecules in the activated samples. The frequencies at 1663 cm^{-1} attributes to the $\nu(\text{CO})$ vibration of the DMF, and the presence of the $\nu(\text{OH})$ stretching frequencies at 1620 cm^{-1} in activated samples may result from the rapid re-adsorption of trace moisture during the IR measurements.

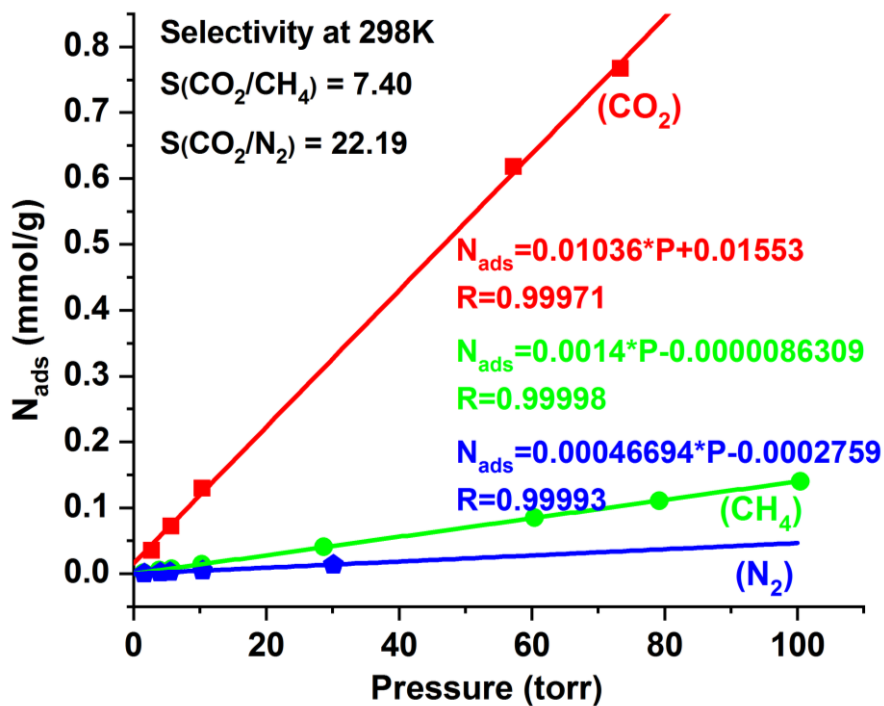


Fig. S5 The fitting initial slope for CO₂, CH₄ and N₂ isotherms for HNUST-9 collected at 298 K (N_{ads} = gases uptake; R = related coefficient). The calculated selectivity of CO₂/CH₄ and CO₂/N₂ for HNUST-9 is about 7.4 and 22.2, respectively.

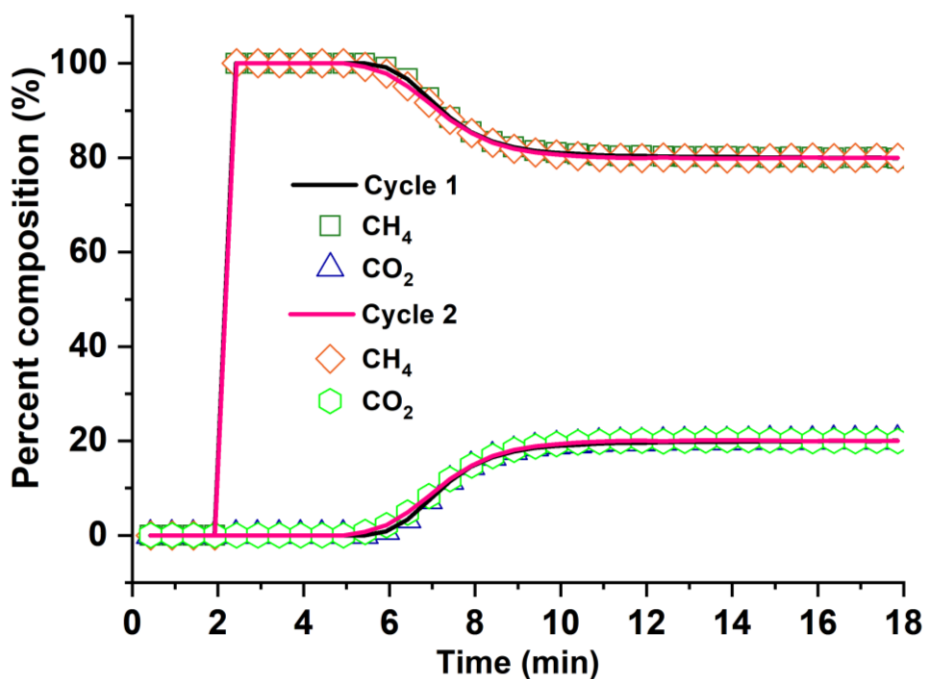


Fig. S6 Repeated CO₂/CH₄ breakthrough experiments of HNUST-9 after 20 min helium gas blowing at 298 K and 1 bar.

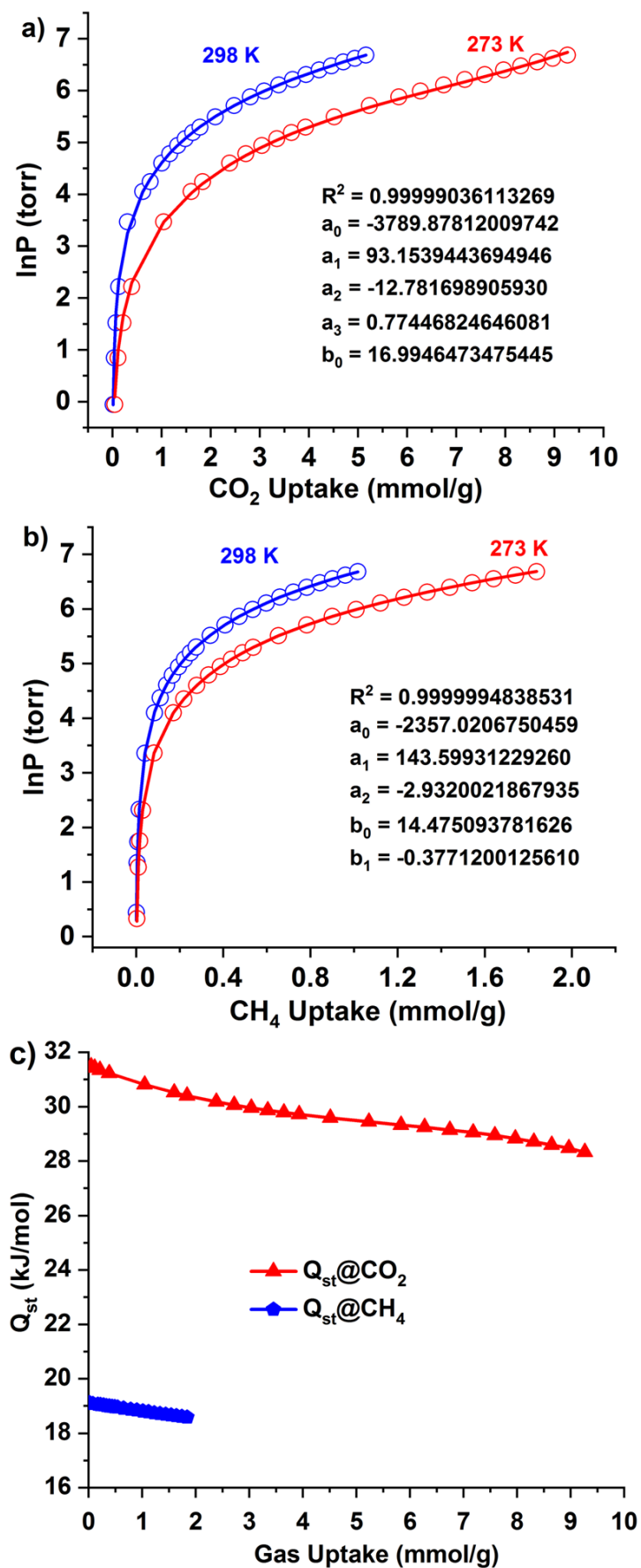


Fig. S7 a-b) Details of Virial equation (symbols) fitting to the experimental CO_2 and CH_4 adsorption data (solid lines) for HNUST-9 collected at 273 K and 298 K; c) The CO_2 and CH_4 isosteric adsorption enthalpies of HNUST-9.

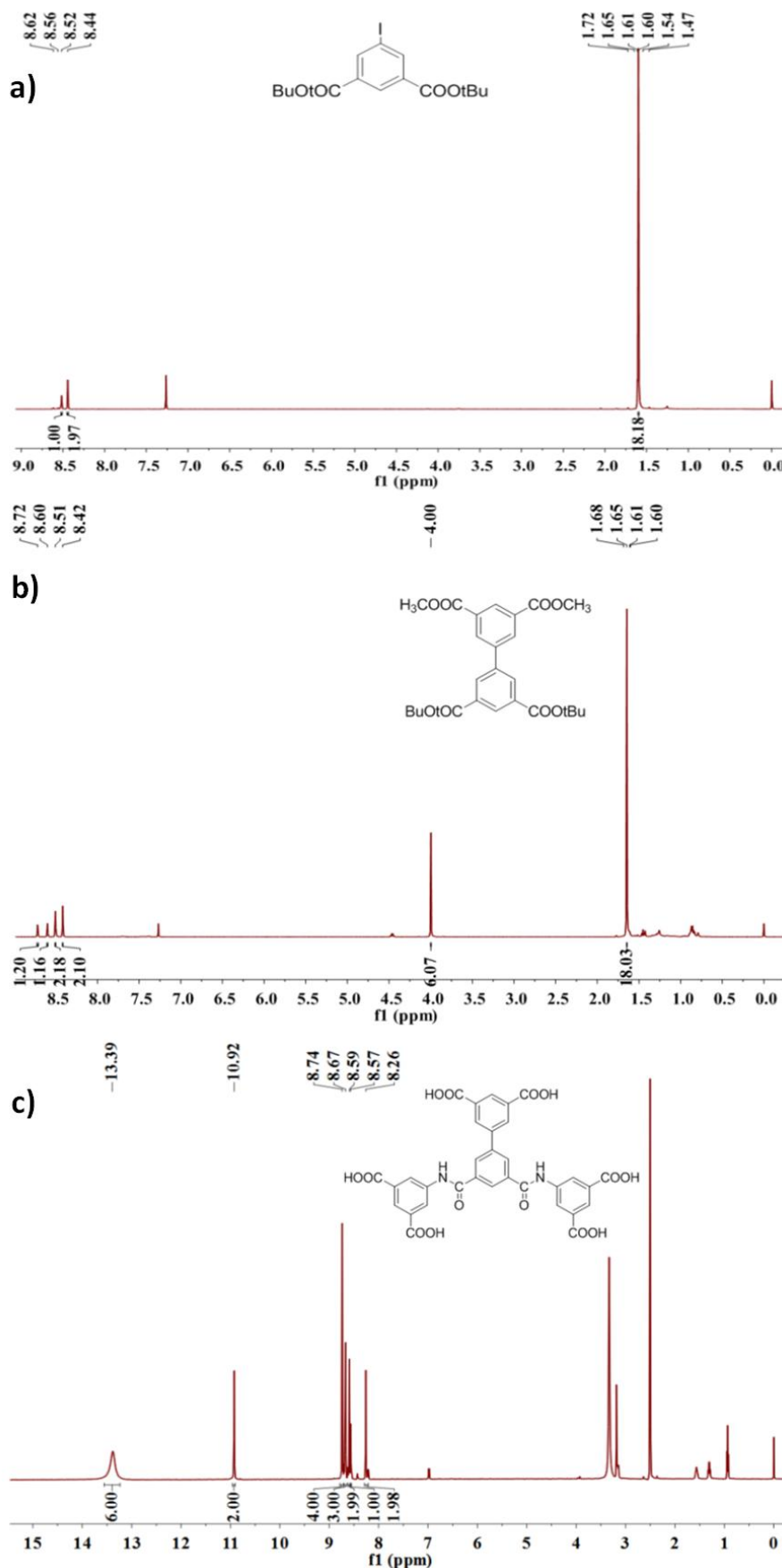


Fig. S8 The ¹H NMR spectrum. a) Di-tert-butyl 5-iodoisophthalate in CDCl₃; b) 3,5-di-tert-butyl 3',5'-dimethyl [1,1'-biphenyl]-3,3',5,5'-tetracarboxylate in CDCl₃; c) H₆DBDBD ligand in DMSO-*d*₆, H₆DBDBD = 5,5'-((3',5'-dicarboxy-[1,1'-biphenyl]-3,5-dicarbonyl)bis(azanediyl))diisophthalic acid.

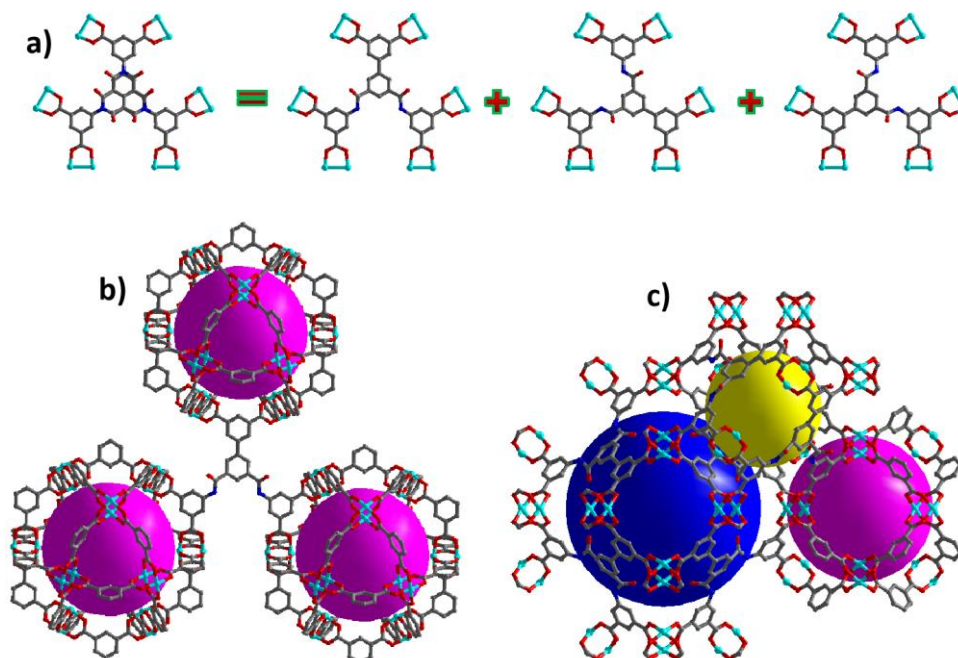


Fig. S9 a) The acylamide and benzene moieties of the DBDBD ligand in the crystal structure of HNUST-9 are disordered over three positions with equal probability; b) A portion of structure of the (3, 24)-connected *rht*-type framework; c) The 3D polyhedra packing in single-crystal structure of HNUST-9. Water molecules and H atoms have been omitted for clarity.

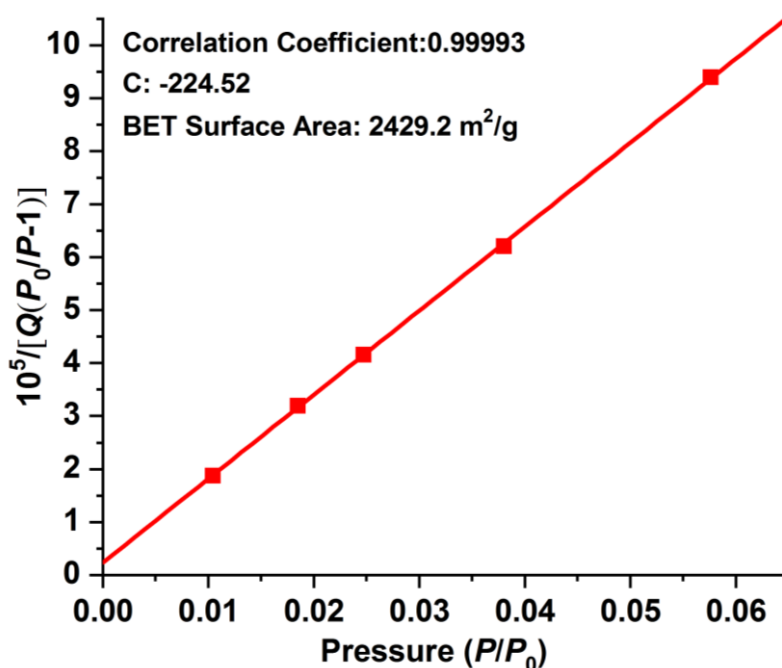


Fig. S10 The BET plots for HNUST-9 in the chosen range ($P/P_0 = 0.01-0.06$). This range was chosen according to two major criteria established in literatures [(a) J. Rouquerol, P. Llewellyn and F. Rouquerol, *Stud. Surf. Sci. Catal.*, **2007**, 160, 49-56; (b) K. S. Walton and R. Q. Snurr, *J. Am. Chem. Soc.*, **2007**, 129, 8552 -8556.]: (1) The pressure range selected should have values of $Q(P_0-P)$ increasing with P/P_0 . (2) The y intercept of the linear region must be positive to yield a meaningful value of the C parameter, which should be greater than zero.

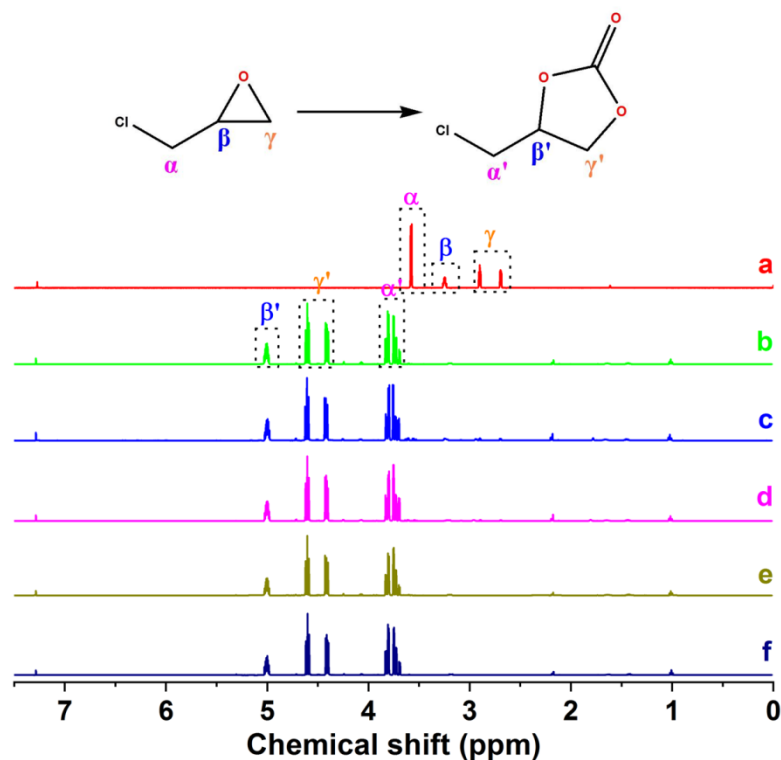


Fig. S11 The ^1H NMR spectrum (in CDCl_3) of a solution after the cycloaddition of CO_2 with 2-(chloromethyl)oxirane: a) without catalyst, b) first cycle, c) second cycle, d) third cycle, e) fourth cycle and f) fifth cycle. The yields of the reaction have been calculated by integration of cyclic carbonates protons at the end of the reaction, due to the distinct chemical shifts for the corresponding epoxide protons.

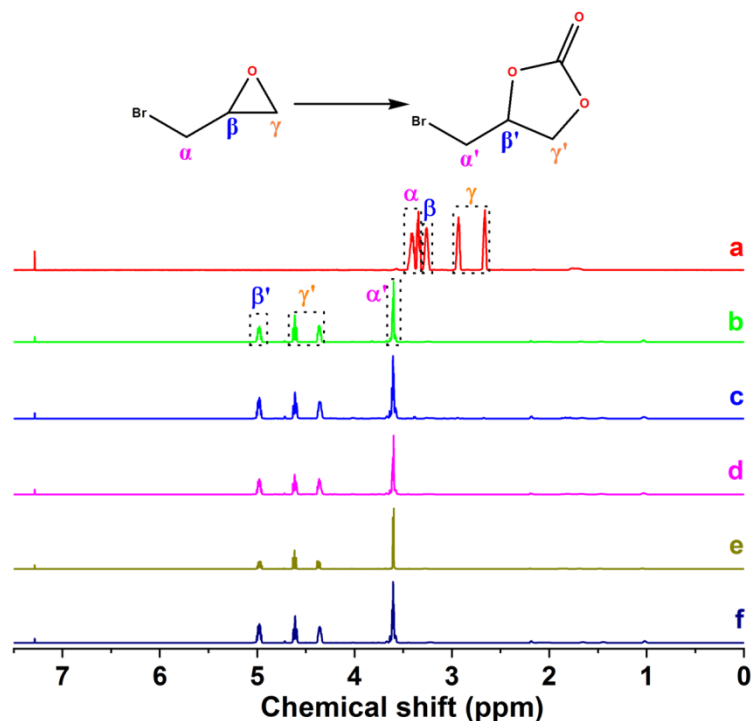


Fig. S12 The ^1H NMR spectrum (in CDCl_3) of a solution after the cycloaddition of CO_2 with 2-(bromomethyl)oxirane: a) without catalyst, b) first cycle, c) second cycle, d) third cycle, e) fourth cycle and f) fifth cycle.

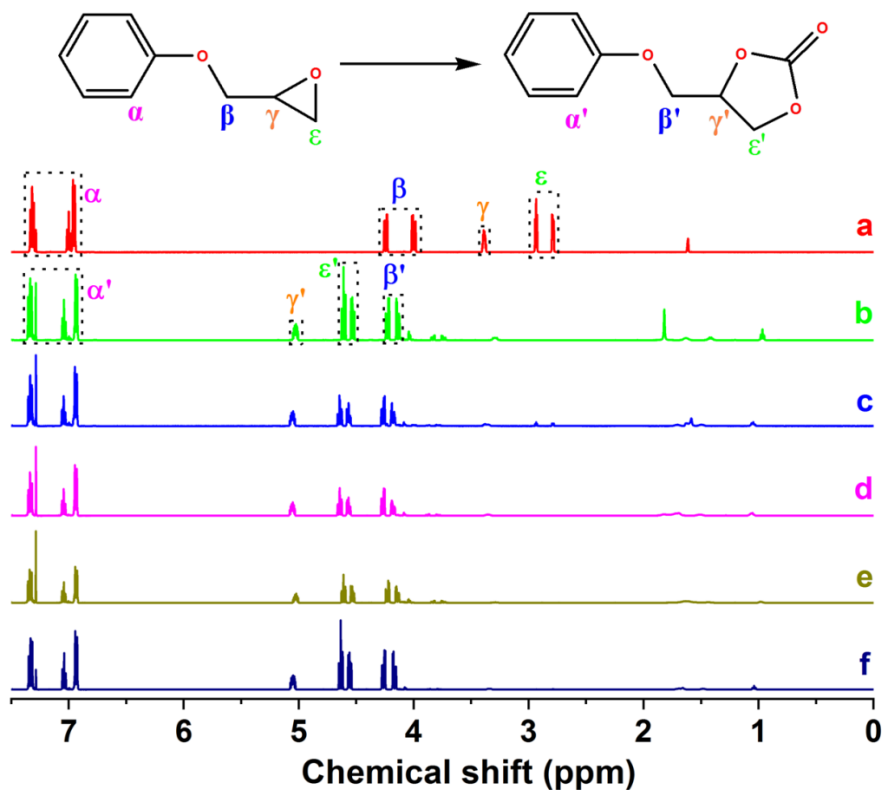


Fig. S13 The ¹H NMR spectrum (in CDCl₃) of a mixture after the cycloaddition of CO₂ with 2-(phenoxymethyl)oxirane: a) without catalyst, b) first cycle, c) second cycle, d) third cycle, e) fourth cycle and f) fifth cycle.

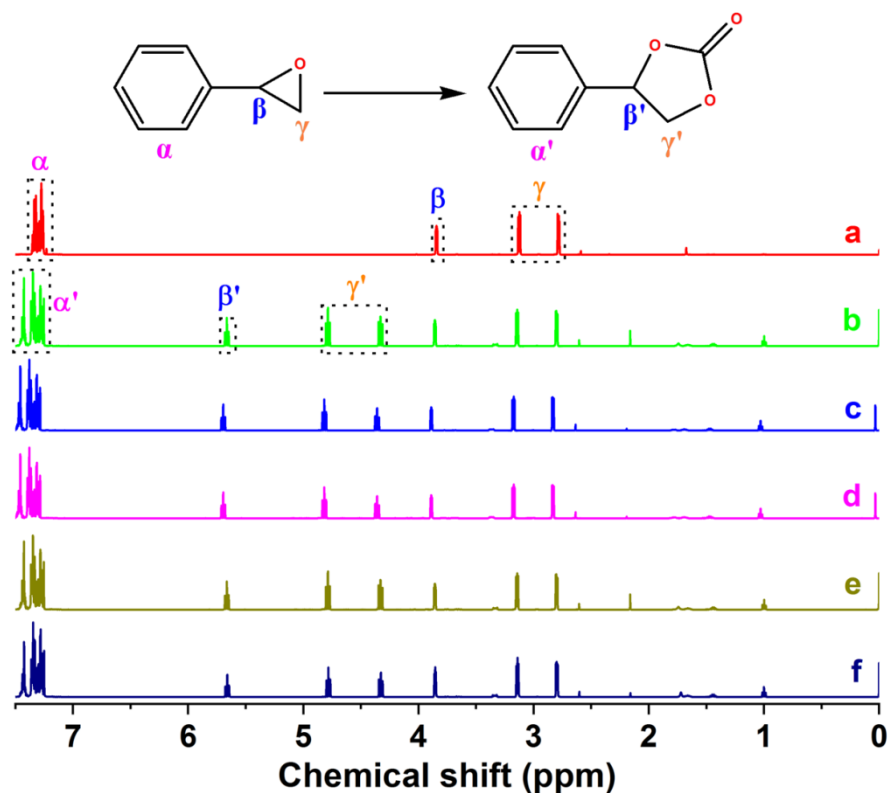


Fig. S14 The ¹H NMR spectrum (in CDCl₃) of a solution after the cycloaddition of CO₂ with 2-phenyloxirane: a) without catalyst, b) first cycle, c) second cycle, d) third cycle, e) fourth cycle and f) fifth cycle.

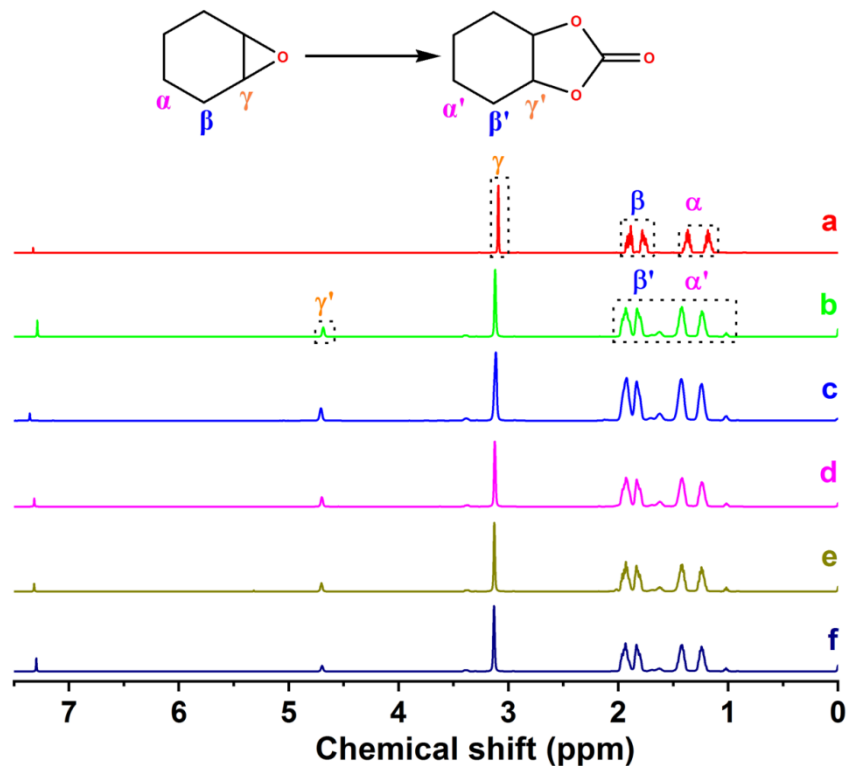


Fig. S15 The ^1H NMR spectrum (in CDCl_3) of a solution after the cycloaddition of CO_2 with cyclohexene oxide: a) without catalyst, b) first cycle, c) second cycle, d) third cycle, e) fourth cycle and f) fifth cycle.

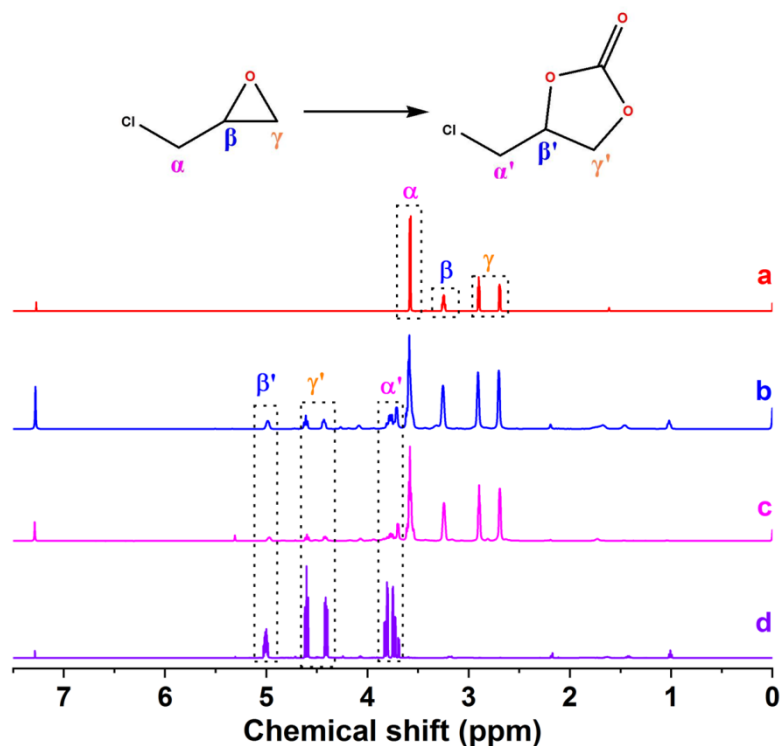


Fig. S16 The ^1H NMR spectrum (in CDCl_3) of a solution after the controlled experiments for cycloaddition of CO_2 with 2-(chloromethyl)oxirane. a) without catalyst, b) catalyzed by the cocatalyst TBAB alone, c) catalyzed by HNUST-9 only, d) catalyzed by both HNUST-9 and TBAB available at the same conditions.

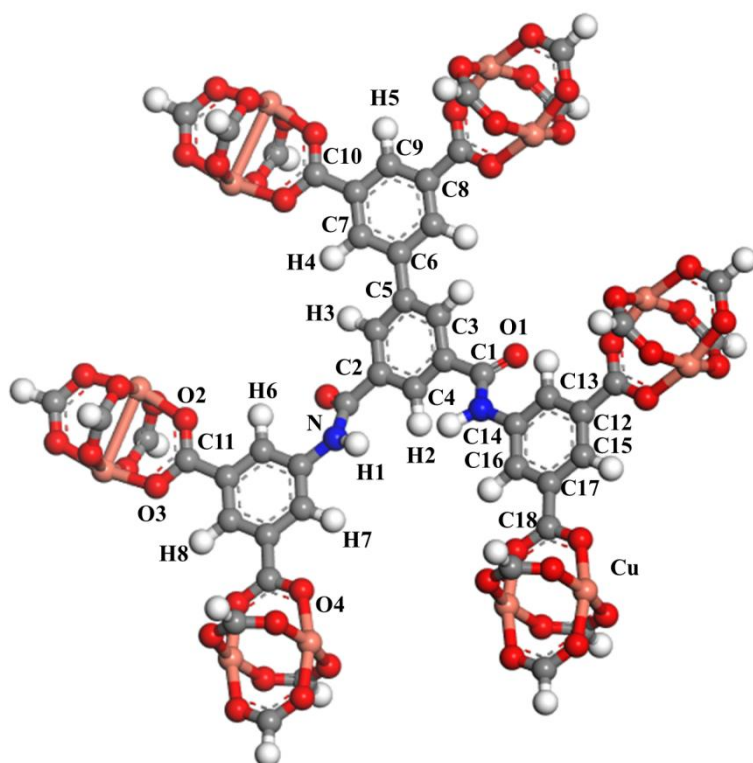


Fig. S17 The atomic schemes in framework of HNUST-9 used for GCMC and First-principles calculations.

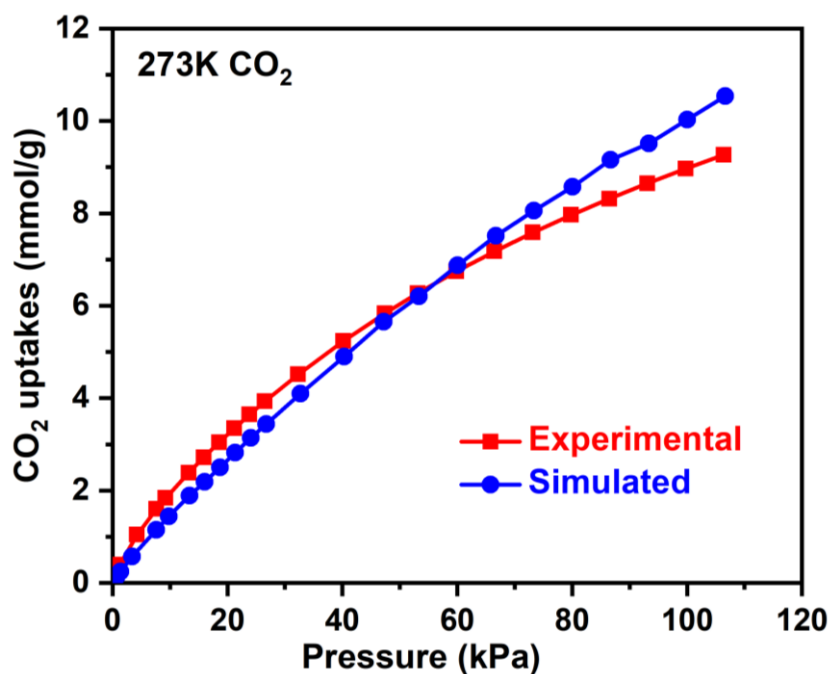


Fig. S18 Comparison of CO₂ adsorption isotherms of HNUST-9 at 273 K up to 1 bar between GCMC simulated and experimental data.

Table S1. Crystal data and structure refinement for HNUST-9.

Identification code	HUNST-9
CCDC number	1836745
Empirical formula	C ₃₂ H ₂₀ Cu ₃ N ₂ O ₁₇
Formula weight	895.14
Temperature	295(2) K
Wavelength	0.71073 Å
Crystal system	Cubic
Space group	Fm-3m
Unit cell dimensions.	$a = b = c = 40.209(9)$ Å, $\alpha = \beta = \gamma = 90^\circ$
Volume	65010(44) Å ³
Z	32
Density (calculated)	0.732 g cm ³
Absorption coefficient	0.813 mm ⁻¹
F(000)	14368.0
Crystal size	0.25 × 0.23 × 0.20 mm ³
2theta range for data collection	4.416 to 50.714
Limiting indices	-43 ≤ h ≤ 48, -48 ≤ k ≤ 42, -48 ≤ l ≤ 48
Reflections collected / unique	154811/2940 [R _{int} = 0.1442]
Completeness	99.5% (2theta = 52.00 °)
Absorption correction	Semi-empirical from equivalents
Refinement method	Full-matrix least-squares on F ²
Data / restraints / parameters	2940/89/123
Goodness-of-fit on F ²	1.189
Final R indices [I > 2σ(I)]	R ₁ = 0.0815, wR ₂ ^a = 0.2444
R indices (all data)	R ₁ = 0.1035, wR ₂ ^a = 0.2802
Largest diff. peak and hole	1.41/-0.74 e. Å ⁻³

$$^a R_1 = \frac{\sum ||F_o| - |F_c||}{\sum |F_o|}; wR_2 = \left[\frac{\sum w(\sum F_o^2 - F_c^2)^2}{\sum w(F_o^2)^2} \right]^{1/2}.$$

Table S2. Lennard-Jones parameters of HNUST-9

Atom Type	ϵ/k_B (K)	σ (Å)	Atom Type	ϵ/k_B (K)	σ (Å)
H	22.141	2.571	C	52.836	3.431
O	30.192	3.118	N	34.721	3.261
Cu	2.516	3.114			

Table S3. Lennard-Jones parameters and charges of adsorbates

Atom Type	ϵ/k_B (K)	σ (Å)	q (e)
CO2_O	80.507	3.033	-0.3256
CO2_C	28.129	2.757	0.6512

Table S4. All partial atomic charges for the MOF material HNUST-9 used in GCMC simulations.

Atom Type	q (e)	Atom Type	q (e)
C1	0.698	C10	0.786
C2	-0.077	C11	0.810
C3	-0.107	C12	0.439
C4	-0.109	C13	-0.216
C5	0.087	C14	-0.028
C6	0.027	C15	0.247
C7	0.079	C16	-0.107
C8	-0.071	C17	-0.045
C9	-0.048	C18	0.820
H1	0.319	H5	0.114
H2	0.097	H6	0.178
H3	0.101	H7	0.165
H4	0.112	H8	0.124
O1	-0.511	O3	-0.679
O2	-0.700	O4	-0.713
N	-0.720	Cu	1.076